

# Sensitivity and specificity for detecting basal cell carcinomas in Mohs excisions with confocal fluorescence mosaicing microscopy

Daniel S. Gareau<sup>\*,†</sup>

Memorial Sloan-Kettering Cancer Center  
Dermatology Service, Room 230  
160 East 53rd Street  
New York, New York 10022  
E-mail: dan@dangareau.net

Julie K. Karen<sup>†</sup>  
Stephen W. Dusza

Marie Tudisco  
Kishwer S. Nehal<sup>‡</sup>  
Milind Rajadhyaksha<sup>‡</sup>

Memorial Sloan-Kettering Cancer Center  
Dermatology Service  
60 East 53rd Street  
New York, New York 10022

**Abstract.** Recent studies have demonstrated the ability of confocal fluorescence mosaicing microscopy to rapidly detect basal cell carcinomas (BCCs) directly in thick and fresh Mohs surgical excisions. Mosaics of confocal images display large areas of tissue with high resolution and magnification equivalent to  $2\times$ , which is the standard magnification when examining pathology. Comparison of mosaics to Mohs frozen histopathology was shown to be excellent for all types of BCCs. However, comparisons in the previous studies were visual and qualitative. In this work, we report the results of a semiquantitative preclinical study in which 45 confocal mosaics are blindly evaluated for the presence (or absence) of BCC tumor. The evaluations are made by two clinicians: a senior Mohs surgeon with prior expertise in interpreting confocal images, and a novice Mohs fellow with limited experience. The blinded evaluation is compared to the gold standard of frozen histopathology. BCCs are detected with an overall sensitivity of 96.6%, specificity of 89.2%, positive predictive value of 93.0%, and negative predictive value of 94.7%. The results demonstrate the potential clinical utility of confocal mosaicing microscopy toward rapid surgical pathology at the bedside to expedite and guide surgery. © 2009 Society of Photo-Optical Instrumentation Engineers. [DOI: 10.1117/1.3130331]

Keywords: Mohs surgery; confocal fluorescence mosaicing microscopy; basal cell carcinoma.

Paper 08285RR received Aug. 13, 2008; revised manuscript received Feb. 13, 2009; accepted for publication Mar. 19, 2009; published online Jun. 24, 2009.

## 1 Introduction

Mohs surgery is superior to conventional skin cancer excision in terms of recurrence rates and cosmetic outcomes, but it is much more difficult. Precise removal of basal cell carcinomas (BCCs) is guided by conventional frozen histopathology. The histopathology must be prepared during surgery and is labor and time consuming, requiring 20 to 45 min for each excision.<sup>1</sup> We have recently shown the ability of large area confocal mosaicing to rapidly detect BCC tumors directly in Mohs surgical skin excisions.<sup>2-4</sup> Using acridine orange to stain nuclear morphology, all types of BCCs such as superficial, nodular, micronodular, and infiltrative are detected.<sup>2</sup> Confocal mosaics that display up to  $12\times 12$  mm of tissue are created and displayed in less than 9 min, with the present laboratory system.<sup>3,4</sup>

Confocal microscopy has been performed in human skin, both *in vivo* as well as in thick specimens *ex vivo* from fresh surgical excisions or biopsies, noninvasively and with subcellular resolution.<sup>5</sup> The noninvasive optical sectioning provided by a confocal microscope serves the same purpose as the

physical sectioning for histopathology. The key difference is the tradeoff between resolution and field of view, which is a well-known constraint in microscopy. A high numerical aperture (NA) is needed for thin optical sectioning, so that cells and nuclei can be resolved but with a correspondingly high magnification, which results in a small field of view. However, a wide field of view is needed to examine pathology. To obtain both thin optical sectioning and wide field of view, large mosaics ( $> 1$  cm) can be constructed by stitching small fields of view ( $< 1$  mm). Confocal mosaics display large areas of tissue with high resolution and low magnification in a manner that is analogous to that seen in thin sections of histopathology.

However, this new imaging mechanism is entirely different and therefore must be validated. The primary aim of this preclinical study was to validate the diagnostic accuracy of confocal fluorescence mosaicing microscopy against the clinical standard of Mohs frozen histopathology. A secondary aim was to determine whether the use of a single stain, such as acridine orange for nuclei, provides the contrast needed to achieve accurate detection of BCCs. This is as opposed to the use of two stains, hematoxylin and eosin (HE) for contrast and countercontrast, which are necessary in histopathology. Confocal mosaics were blindly evaluated and compared to conventional

<sup>†</sup>With equal contribution from the first two authors.

<sup>‡</sup>With equal contribution from the two senior authors.

\*Address all correspondence to Daniel Gareau, Oregon Health & Science University, Mail code: CH13B-3303 SW Bond Avenue, Portland, OR 97239; Tel: 503 708 7078; Fax: 212 308 0854; E-mail: dan@dangareau.net

histopathology with HE staining. We report the results, in terms of sensitivity and specificity, for detecting BCCs with rapid large area confocal fluorescence mosaicing microscopy.

## 2 Materials and Methods

Details of the acquisition and processing of confocal mosaics have been described earlier.<sup>2-4</sup> Discarded skin excisions were obtained after Mohs surgery under an internal review board-approved protocol. The excisions were thawed, rinsed in isotonic saline solution, immersed in 1-mM acridine orange solution for 20 sec, and rinsed again in preparation for confocal imaging.

Acridine orange provides strong and robust nuclear-to-cytoplasm and nuclear-to-dermis contrast.<sup>2</sup> The fluorescence is fairly resistant to photobleaching. With illumination power of 3 to 5 mW on the tissue, the time for fluorescence bleaching (i.e., decrease to 1/3 of its initial power) was determined to be approximately 3 min. This is on the same order of magnitude as 50 sec, which was found by others, but under different experimental conditions.<sup>6</sup> Equally important is that the use of acridine orange does not affect subsequent frozen histopathology, as determined in our previous study.<sup>2</sup>

The Mohs excisions in the study ranged in size from 2 to 20 mm and were, on average, 8.8+/-4.0 mm long and 4.8+/-2.0 mm wide. The aspect ratio (length/width) was 1.8+/-0.4. A specially engineered fixture was used for mounting Mohs surgical excisions in a manner similar to that in cryostats for preparing frozen histopathology sections. Up to 36x36 images were captured, processed for illumination artifacts including vignetting, and stitched with a Matlab-based algorithm to create mosaics.<sup>2</sup> A full mosaic of 36x36 images displays 12x12 mm of the Mohs excision such that the magnification and resolution is equivalent to that of a standard 2x view of histopathology. The mosaics were displayed to the Mohs surgeon on a large monitor with sufficient resolution to mimic that in a standard 2x view of histopathology. Smaller submosaics were displayed with higher magnification and higher resolution at the discretion of the observer. For comparison to the confocal mosaics, the corresponding Mohs frozen histopathology was processed and obtained, as described previously.<sup>2</sup>

48 mosaics were prepared for this study. The excisions included both positive cases with BCC tumor and negative cases without BCC tumor. Normal cases (control) consisted of either excisions from positive cases that were free of tumor (i.e., from the last stage of Mohs surgery), or excisions from negative cases. The positive cases included all types of BCCs such as superficial, nodular, micronodular, and infiltrative. Our Mohs histotechnician (author Tudisco) and one of our investigators (author Gareau) reviewed all the mosaics with the corresponding HE-stained frozen sections for overall quality, to identify cases where tissue disruption or other artifacts would have compromised the correlation to histopathology. Three cases showed gross miscorrelation and were excluded. The remaining 45 mosaics were included along with correlating histopathology. From these 45 mosaics, 149 submosaics were created for evaluation. Each submosaic displayed excisions with magnification as close to 4x as possible. The magnification of 4x was chosen to be the standard for evaluation

of mosaics, considering that the Mohs surgeon examines frozen histopathology with either 2x or 4x.

Figure 1 shows a confocal mosaic that was halved into two submosaics (see solid line) such that each displays with approximately 4x magnification. Larger mosaics of larger excisions were quartered, as necessary, to create four submosaics (as an example, see dotted line in Fig. 1). A few very large mosaics were further divided as necessary.

The evaluation team consisted of a Mohs surgeon (author Nehal) and a Mohs fellow (author Karen). Both evaluated each mosaic independently such that the total number of evaluations was 298. The Mohs surgeon is an expert in interpreting confocal images and mosaics due to several years of involvement in this project. (Her prior experience was, however, mainly in interpreting reflectance confocal mosaics.<sup>3,4</sup>) By comparison, the Mohs fellow was a novice, with only a few months of experience. Both were blinded to the histopathology and the case status (patient information). The evaluations were carried out several weeks after the surgeries, and the reviewers (who had performed the surgeries earlier) had forgotten the diagnosis originally made, because there had been about one hundred cases in the interim. The evaluations were thus blinded.

Submosaics were presented in a random order. The evaluation consisted of a standardized procedure where each submosaic was initially displayed with magnification of approximately 4x, as explained earlier. Submosaics were then "zoomed" and "panned" for careful examination of tissue architecture at higher magnifications of 10 to 30x. The zooming and panning was performed only when necessary, mimicking the process traditionally undertaken during Mohs surgery for rapid examination of frozen histopathology.

Evaluation of each submosaic consisted of identification of the presence or absence of BCC tumors, types of tumors that included superficial, nodular, micronodular, and infiltrative, and "tumor burden" (i.e., amount of tumor). As previously described,<sup>1-4</sup> BCCs were detected based on features such as shape, size, and location of tumor foci, pleomorphism or nuclear atypia, nuclear crowding or increased nuclear density, peripheral palisading, and clefting. The detection of normal skin included features such as eccrine ducts, sebaceous glands, hair follicles, and an epidermis along the periphery of the Mohs excision.

The outcome in this study was the evaluation for the presence or absence of BCC tumor in the submosaics, as compared to the corresponding Mohs frozen histopathology. The evaluation was thus of a binary and semiquantitative nature. The statistics of the comparisons in terms of sensitivity, specificity, positive predictive value, and negative predictive value were determined using binary marginal general linear models. The statistical analyses were performed using Stata SE, version 9.2.

## 3 Results

Of the 149 submosaics, 59.7% (i.e., 89) contained BCC tumor and 40.3% (i.e., 60) did not contain BCC tumor and were of normal skin. The prevalence of BCCs in about 60% of the cases is representative of that typically encountered by Mohs surgeons.

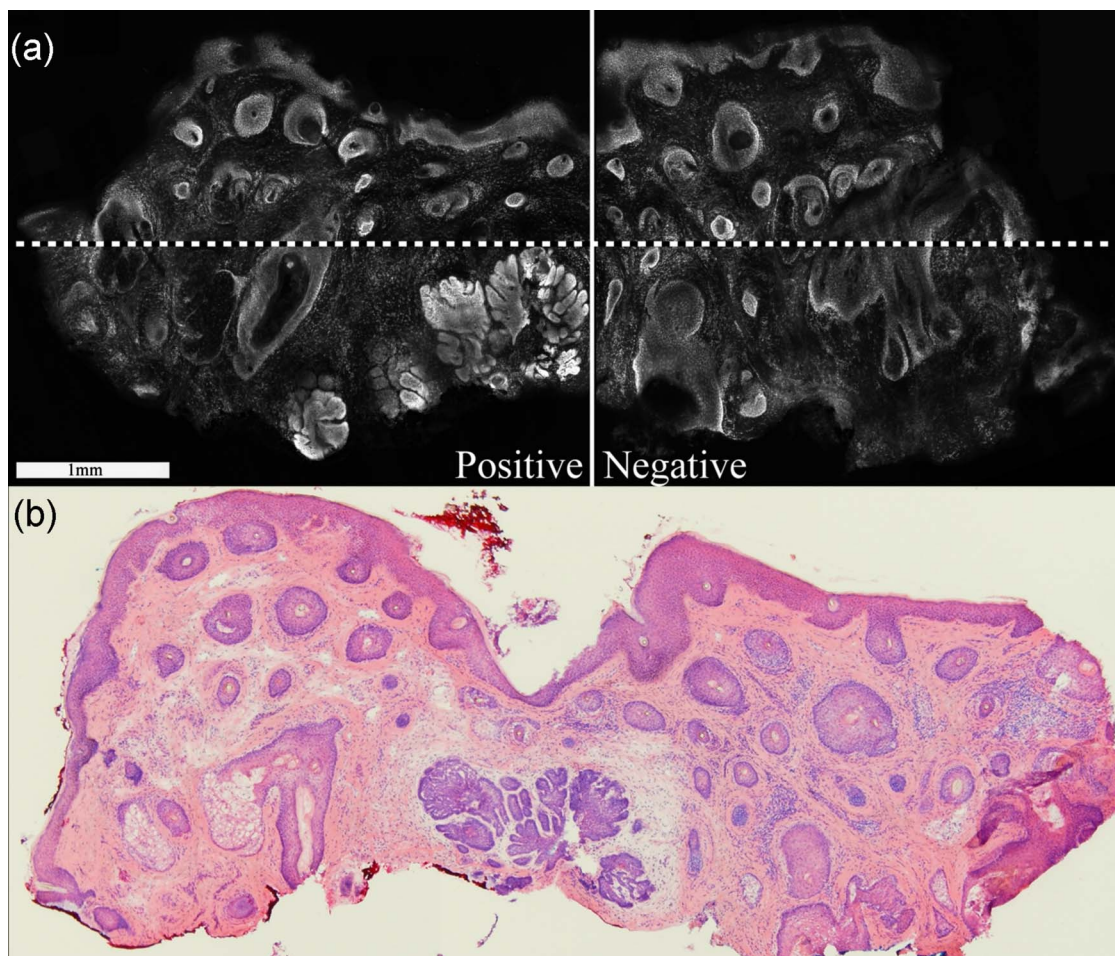


**Fig. 1** (a) Fluorescence confocal mosaic showing nodular BCC, (b) and the corresponding Mohs frozen histopathology. The full mosaic is divided into two submosaics, as shown by the solid white line. The field of view for each submosaic was 3.5 mm, which, in this particular case, was somewhat less than the 5 mm expected for 4 $\times$  magnification. This particular case illustrates both a positive submosaic (i.e., with BCC tumor) and a negative submosaic (i.e., normal tissue without BCC tumor). Larger excisions were divided into quarters to produce submosaics, as indicated, for example, by the additional dashed white line.

Figure 2 shows examples of both normal and malignant features seen in Mohs excisions. Normal skin components such as eccrine glands, sebaceous glands, hair follicles, and epidermis along the periphery of the excision were identified by monomorphic, well-ordered nuclear structure. Malignant features in BCC tumors such as nuclear crowding, pleomorphism, overall disarray of organization, as well as architectural features such as peripheral palisading and clefting, were also identified.

Table 1 summarizes the results of the statistical evaluation of the blinded comparison of confocal mosaics to the gold standard of corresponding Mohs frozen histopathology.

The subtle types of BCC tumor, which are mainly infiltrative and superficial, accounted for most of the false negatives. Small or tiny infiltrative BCC tumors were challenging to detect due to their diminutive size relative to the surrounding dermis. Figure 3 illustrates a case where a large number of infiltrative BCC tumors facilitated easy identification of the cluster. However, in cases with a sparse number and no obvious clusters, identification was relatively more difficult.

Figure 4 shows a superficial BCC tumor that was missed

by both the Mohs surgeon and the Mohs fellow. The inset in Fig. 4(a) shows the subtle but specific characteristic of tumor growth including nuclear crowding, peripheral palisading, and leaf-like projections from the epidermis. Superficial tumors were difficult to detect in mosaics where the edge of the excision was not entirely visualized. Superficial BCC tumors were challenging even in mosaics with perfect display of edges. This is because the tumors extend contiguously from the epidermis at the periphery of the Mohs excision [see Fig. 4(a) inset], such that the overall brightness of the tumor was not significantly greater than the adjacent normal tissue.

Furthermore, the tissue fixture occasionally failed to press the edges of the Mohs excision flat against the optical window (coverslide) of the microscope, leading to incomplete imaging of the epidermis along the periphery. Superficial BCC may be missed if the imaging of the epidermal margin is incomplete. In Fig. 4(a), the confocal submosaic shows missing epidermis due to incomplete compression of the edges of the excision in the tissue fixture. By comparison, the epidermis is completely seen in the histopathology in Fig. 4(b).

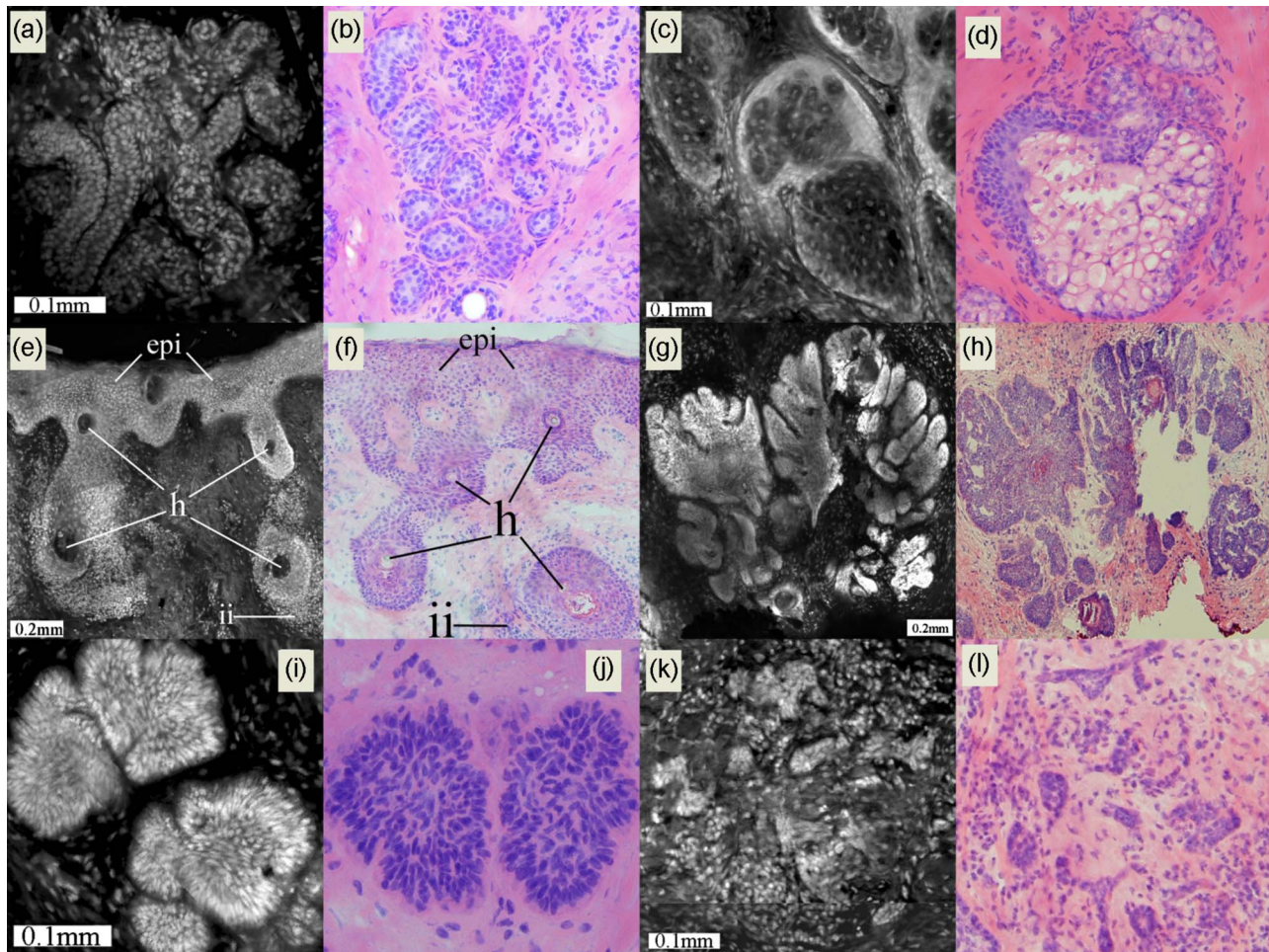


**Fig. 2** Examples of morphological features as seen in confocal fluorescence submosaics and the corresponding Mohs frozen histopathology. In each pair of images, the left one is the confocal and the right is the histopathology. Benign features are: (a) and (b) eccrine gland, (c) and (d) sebaceous gland, (e) and (f) epidermis (epi) along the periphery of the Mohs excisions containing hair follicles (h), along with lymphocytic inflammatory infiltrate (ii) in the deeper surrounding dermis. Malignant features are: (g) and (h) nodular BCC tumor, (i) and (j) micronodular BCC tumor, and (k) and (l) infiltrative BCC tumor.

**Table 1** Results of the statistical evaluation of the blind comparison of confocal mosaics to the corresponding Mohs histopathology. For the two reviewers combined, there were six false positives and 13 false negatives. There was no difference in sensitivity between the two reviewers ( $p$ -value=0.096). There was a borderline difference in specificity between the two, with the Mohs fellow performing at a higher level of specificity than the Mohs surgeon ( $p$ -value=0.056).

Statistical parameter	Mohs surgeon (expert)	Mohs fellow (novice)	Overall estimate	95% confidence interval	
				Upper	Lower
Sensitivity	98.9%	94.4%	96.6%	98.7%	92.8%
Specificity	83.3%	95.0%	89.2%	94.1%	82.2%
Positive predictive value	89.8%	96.5%	93.0%	96.2%	88.3%
Negative predictive value	98.0%	91.9%	94.7%	98.0%	88.8%

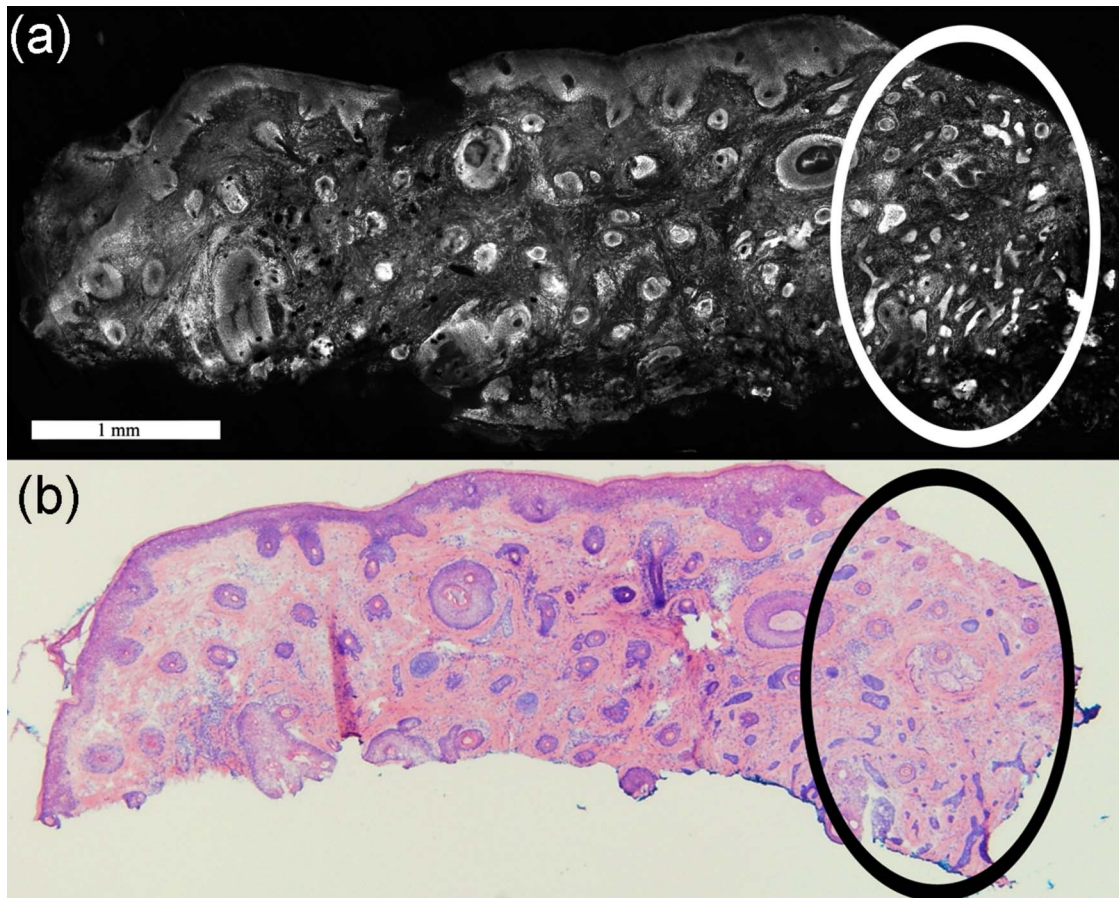


**Fig. 3** Small infiltrative BCCs are differentiated from normal features such as (a) hair follicles in the confocal mosaic, as validated by (b) the corresponding histopathology. Enclosed in the dotted circle is the cluster of infiltrative tumors. The large cluster in this case made the tumors easily identifiable.

#### 4 Discussion

The results of this preclinical study establish, objectively and quantitatively, the feasibility of confocal mosaicing microscopy to rapidly detect BCC tumors in Mohs surgical excisions. With the use of stable contrast agents that allow rapid staining of tumors without photobleaching, this technology may be advanced into clinical trials toward bringing pathology to the bedside with high sensitivity and specificity. The remaining technological advance toward clinical trials is to engineer a tissue fixture for complete and repeatable imaging. This is especially necessary for detection of superficial BCC tumors that extend from the epidermis into the dermis, such that the fixturing must include the epidermal margins along the edges of the excision. Provided that the entire epidermal margin can be imaged with 100% repeatability, the confocal mosaic may offer diagnostic value that can significantly expedite Mohs histopathology.

The fluorescence signal and visual contrast of nuclear morphology and image quality of the mosaics are excellent, as qualitatively and independently assessed by the Mohs surgeon and Mohs fellow. The qualitative criteria for image quality were appearance for seamless and contiguous stitching, appearance of resolution and sharpness, and appearance of contrast. The artifact produced by mosaic stitching was small and not distracting in more than 90% of the mosaics. The contrast

of nuclei over the background dermis was good (10 to 100 fold), as assessed previously.<sup>2</sup> The visual comparison of mosaics to histopathology shows that acridine orange is an effective contrast agent for consistent staining of nuclei for detecting BCC tumors. This confirms the qualitative results from our previous study.<sup>2</sup> Furthermore, the results of the statistical evaluation show that a single nuclear stain may be adequate for detecting BCC tumors.

Both the Mohs surgeon (expert) and Mohs fellow (novice) noted that the examination of confocal mosaics and submosaics was similar to the routine examination of their histopathology—rapid observation of BCC tumor and normal tissue architecture at low magnification (2 to 4 $\times$ ) and low resolution followed, when needed, by further inspection of nuclear morphology at higher magnification (10 $\times$ ) and higher resolution. Examining submosaics at 4 $\times$  magnification was usually adequate for detecting BCC tumors based on the morphology and strong fluorescence contrast relative to the surrounding normal tissue. Questionable cases were further examined at higher magnification of, usually, 10 $\times$ , and only very occasionally up to 30 $\times$ , to allow inspection of nuclear morphology. Overall, the correlation between the confocal submosaics and the Mohs histopathology was good for the location and morphology of BCC tumors, details of nuclear morphology, and amount of tumor or tumor burden. All the

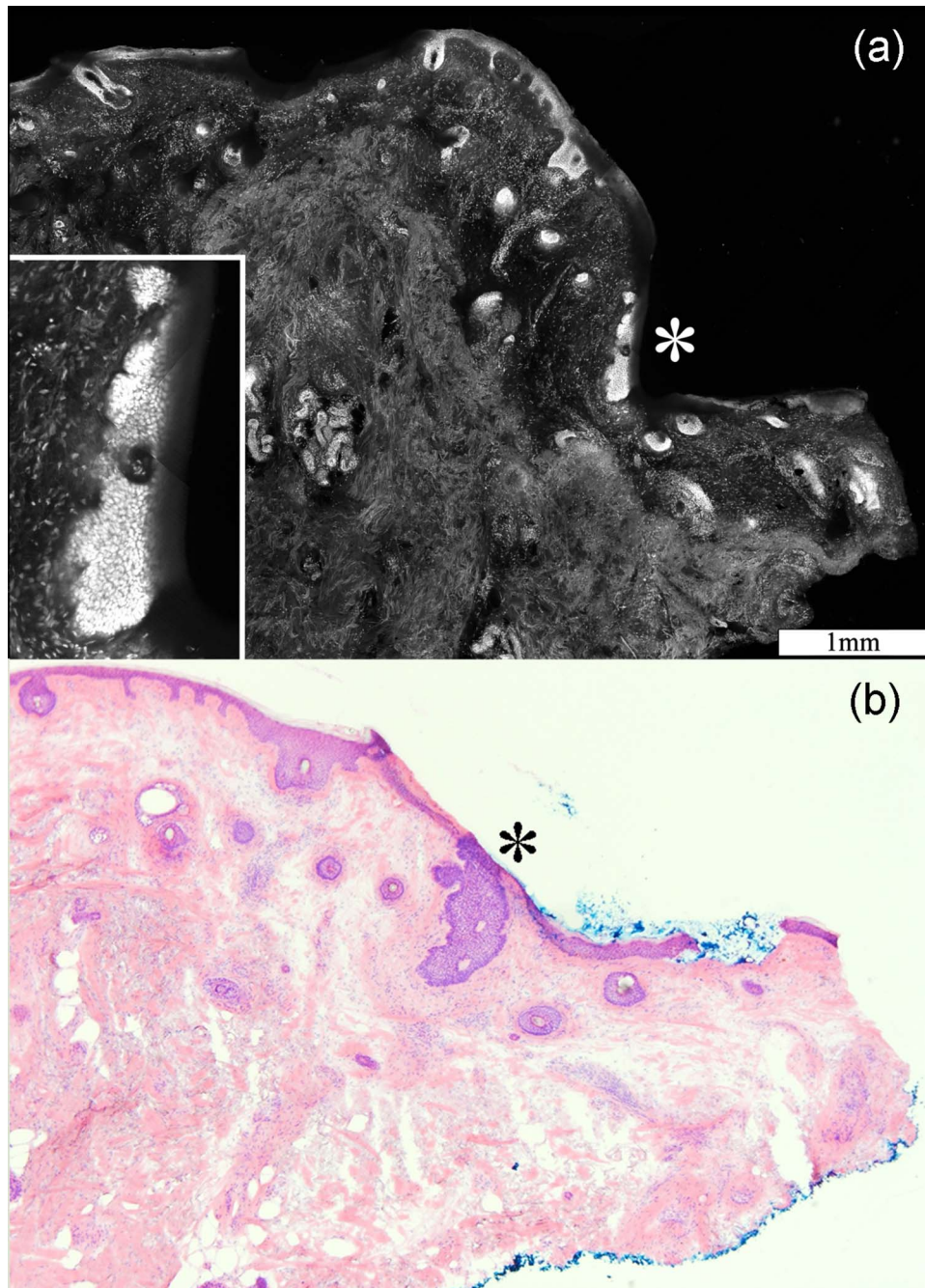


**Fig. 4** Superficial BCC tumor extending contiguously from the epidermis along the periphery of the Mohs excision, as seen in (a) the confocal mosaic and (b) corresponding histopathology. The inset, at high magnification, shows nuclear crowding, peripheral palisading, and leaf-like projections from the epidermis.

major types of BCCs were identifiable. These include superficial, nodular, micronodular and infiltrative.

The interpretation of mosaics was easy for nodular and micronodular BCCs, but relatively more challenging for superficial and infiltrative BCCs. The same challenges are experienced by Mohs surgeons when interpreting histopathology. The challenges were due to an incomplete epidermal margin (for superficial BCCs), presence of dense inflammatory infiltrates that may obscure tumors (especially infiltrative BCCs), and saturated artifacts that appeared as tumor due to excess

dye accumulation. However, as the study progressed, the sensitivity and specificity improved for both Mohs reviewers, suggesting a learning curve—but a reasonably quick one—for interpreting confocal mosaics. Of note, the Mohs fellow who was a novice and completely new at interpreting confocal mosaics was able to learn within a few sessions. The Mohs surgeon was interpreting the fluorescence mosaics in a blinded manner for the first time, but was an expert with the benefit of several years of experience. The prior experience, however, was in evaluating mosaics mainly in reflectance

contrast (using acetic acid for nuclear contrast). Her experience evolved as a clinical coinvestigator during the earlier years of this project. While this experience enabled the Mohs surgeon to learn to interpret fluorescence mosaics fairly easily, the novice with limited prior experience was relatively quick, too. Interested readers are invited to view our mosaics and analyze the results from this study via the Internet.<sup>7</sup>

In this preclinical study, we tested mosaicing technology only for detecting BCCs, since these account for more than 80% of all skin cancers. A follow-up preclinical study will be necessary to test the detectability of squamous cell carcinomas (SCCs). SCCs are the other main type of tumors that are removed by Mohs surgery, but these occur in much smaller numbers compared to those of BCCs. For SCCs, especially the invasive type that requires examination of cellular cytoplasm and keratinization, an alternate contrast agent such as eosin may be more effective. Thus, although single stains such as acridine orange for nuclei or eosin for cells may be effective for detecting individual types of tumors such as BCCs or SCCs, respectively, the use of multiple stains or a multimodal combination of contrast agents may be necessary for truly successful implementation in the clinic.

With the current laboratory system, the acquisition-and-display time for a typical mosaic is up to 9 min for the largest excisions.<sup>3,4</sup> (Smaller excisions require 5 min or less.) Preliminary engineering analysis estimates that, with modest improvement in hardware and software, mosaicing of up to 20 × 20 mm of tissue may be possible in 2 to 3 min. The use of the laboratory system including staining of the Mohs excision, the use of the tissue fixture for mounting, and the creation of mosaics is straightforward, as experienced by two second-year medical summer students. Each spent two months and learned to operate the system in a few days. Thus, we believe that the remaining challenges are not in technology but in further development of contrast agents. Future work aims to develop single- and multimodal-contrast mechanisms in a wider range of tissues from excisions of oral mucosal lesions, thyroid nodules, parathyroid glands, and bone during head-and-neck surgery, needle core biopsies and lumpectomies of breast, and preoperative biopsies of the liver, bladder, and other tissues.

Confocal imaging allows rapid 3-D interrogation of tissue. In this study, the mosaics were reviewed off-line, after the

imaging sessions, so there were no real-time observations made in depth. However, live mosaicing may be envisioned for rapid examination of pathology in 3-D at the bedside. Thus, confocal mosaicing microscopy may evolve into an attractive adjunct or alternative to frozen histopathology, and shows promise to expedite not only Mohs surgery but any procedure based on sequentially staged excisions and/or requiring immediate pathology. Rapid and noninvasive pathology may be possible to save time and cost associated with surgical procedures.

#### Acknowledgments

The authors thank Mohs technician Barbara Strippoli for supplying discarded excisions from Mohs surgeries, help with the frozen histopathology, and intellectual involvement with this research. Essential technical support was provided by Jay Eastman and William Fox of Lucid Incorporated. This research was funded by NIH grant R01EB002715 from the Image-Guided Interventions program of the NIBIB (program officer John Haller), and by a grant from the Byrne Fund, Department of Medicine at MSKCC.

#### References

1. M. Rajadhyaksha, G. Menaker, T. J. Flotte, P. J. Dwyer, and S. Gonzalez, "Rapid confocal examination of non-melanoma cancers in skin excisions to potentially guide Mohs micrographic surgery," *J. Invest. Dermatol.* **117**, 1137–1143 (2001).
2. D. S. Gareau, Y. Li, B. Huang, Z. Eastman, K. S. Nehal, and M. Rajadhyaksha, "Confocal mosaicing microscopy in Mohs skin excisions: feasibility of rapid surgical pathology," *J. Biomed. Opt.* **13**(5), 054001 (2008).
3. Y. P. Patel, K. S. Nehal, I. Aranda, Y. Li, A. C. Halpern, and M. Rajadhyaksha, "Confocal reflectance mosaicing of basal cell carcinomas in Mohs surgical skin excisions," *J. Biomed. Opt.* **12**(3), 034027:1–10 (2007).
4. D. S. Gareau, Y. G. Patel, Y. Li, I. Aranda, A. C. Halpern, K. S. Nehal, and M. Rajadhyaksha, "Confocal mosaicing microscopy in skin excisions: A demonstration of rapid surgical pathology," *J. Microsc.* **233**(1), 149–159 (2009).
5. *Reflectance Confocal Microscopy of Cutaneous Tumors—An Atlas with Clinical, Dermoscopic and Histological Correlations*, S. G. Gonzalez, M. Gill, and A. C. Halpern, Eds., Informa Healthcare, London (2008).
6. D. M. Benson, J. Bryan, A. L. Plant, A. M. Gotto, and L. C. Smith, "Digital imaging fluorescence microscopy: spatial heterogeneity of photobleaching rate constants in individual cells," *J. Cell Biol.* **100**, 1309–1323 (1985).
7. See <http://www.dangareau.net/mohs08/index.html>.